Effect of Strongly Coupled Plasma on the Spectra of Hydrogenlike Carbon, Aluminium and Argon

S. Bhattacharyya[1], A. N. Sil[2,4], S. Fritzsche[3], P. K. Mukherjee[4]

[1]Kandi Raj College,
Kandi, Murshidabad, West Bengal 742 137, India

[2]Max Planck Institute for the Physics of Complex Systems,
Nöthnitzer Str. 38, D-01187 Dresden, Germany

[3] Universität Kassel,
Institut für Physik, 34109 Kassel, Germany

[4] Indian Association for the Cultivation of Science,
Jadavpur, Kolkata-700 032, India

April 11, 2007

Abstract

A detailed study has been performed for estimating the orbital energies, positions and shifts of the Lyman lines of C^{5+}, Al^{12+} and Ar^{17+} under strongly coupled plasma with a view to understand such line positions and shifts obtained in laser produced plasma experiments. The effect of strongly coupled plasma has been treated within the Ion Sphere (IS) model. Both non-relativistic and relativistic methods have been used for estimating the spectral properties. Theoretical estimates with IS model of the plasma are in conformity with the results of laser plasma experiments on these highly stripped ions. The experimental data for the systems have also been compared with the theoretical estimates using Debye screening model of the plasma with spatial confinements which gives additional restrictions to the wave functions at finite boundaries.

1 Introduction

The spectral properties of atomic systems are modified considerably under external confinements [1, 2, 3]. Of particular interest, is the effect of a surrounding plasma of different coupling strengths Γ, defined as the ratio of average Coulomb potential energy between pairs of particles and their kinetic energy. $\Gamma < 1$ for weakly coupled plasma, one can apply the standard Debye screening model [4] in which the potential energy between charged particles is represented by a screened Coulomb potential. The condition $\Gamma \geq 1$ refers to strongly coupled plasma in which the potential energy function, though simple, is of completely different nature than in a Debye screening model [5]. Such plasma conditions prevail in, highly evolved stars, the interior of Jovian planets, explosive shock tubes, two dimensional states of electrons trapped in surface states of liquid helium, laser produced and inertial confinement fusion plasmas [5, 6]. Recent experimental observations using laser produced plasmas [7, 8, 9, 10, 11, 12] open up an interesting field for the theoretical investigations along this line. Such high density plasmas are of particular interest in astrophysics and inertial confinement fusion processes. The X-ray opacity of matter under stellar interior conditions and the X-ray diagnostics of ICF plasmas can be achieved from such a study [11]. Effect of dense plasma on the ionization potential, collision and photo absorption cross sections, fine structure splitting and spectral line shifts have been investigated earlier by Stewart and Pyatt [13], Rozsnai [14], Ray [15], Jung [16], Griem [17], Siedel *et al.* [18] and Skupski [19]. Applications of density functional approach along this line was reviewed by Gupta and Rajagopal [20].

In the current context, we will focus our attention to the experimental findings based on time and space resolved extreme ultraviolet spectra of Carbon plasmas with 100 fs laser pulses [10], inertially confined laser imploded Ar plasma [11] and ultrashort laser produced Al plasma [12]. For such laser produced plasmas $\Gamma > 1$ and one can apply strongly coupled plasma model to investigate the spectral properties of isoelectronic ions of Hydrogen. In this communication we would like to investigate in detail the effect of strongly coupled plasma on the Lyman lines of highly stripped Carbon, Aluminium and Argon. Ion Sphere (IS) model of the plasma [5] has been utilized for such a study. Our motivation is to investigate how the simple IS model is effective in obtaining results which can be compared favourably with the experimentally observed values. In addition we would also like to investigate the applicability of the Debye plasma model with a spherical confinement on the spectral line positions and shifts of the Lyman lines under the laser plasma experimental conditions [10, 11, 12] and to estimate the shifts in ionization potentials. Such studies have been done earlier for Hydrogen [21, 22] and Helium like systems [23, 24] to understand the behavior of the structural properties of one and two electron systems under weak as well as strongly coupled plasmas. A brief outline of the theory is given in Section 2 and a discussion of the results follow in Section 3.

2 Theory

In presence of an external plasma environment the potential energy is modified and the non-relativistic Hamiltonian of a Hydrogen like atomic system [a.u. is used throughout] can be represented by

$$H_0 = -\frac{1}{2}\nabla^2 + V_{eff}(r) \tag{1}$$

where the structure of the one body effective potential depends on the type of the coupling of the plasma with the atomic charge cloud. For the relativistic treatment appropriate modification of the Hamiltonian is done through the introduction of the Dirac operators. Currently we are interested in the case of strongly coupled plasma for which $\Gamma \geq 1$. In case of such a homogeneous one component plasma surrounding an ion of nuclear charge Z having one valence electron, one can define a sphere of radius R (usually referred to as the Wigner-Seitz radius) such that the plasma electrons with density n together with the valance electron completely neutralize the central positive charge; thus maintaining the overall charge neutrality of the system [5, 13, 20]. In such a situation the Wigner-Seitz radius R is given by

$$R = \left[\frac{(Z-1)}{\frac{4}{3}\pi n}\right]^{\frac{1}{3}} \tag{2}$$

From classical electrostatics one can easily obtain

$$V_{eff}(r) = -\frac{Z}{r} + \frac{(Z-1)}{2R}\left[3 - \left(\frac{r}{R}\right)^2\right] \tag{3}$$

In order to analyze the energy of the system for different coupling strengths of the plasma reflected in R, one has to solve the appropriate Schrödinger equation

$$H_0\psi = E_0\psi \tag{4}$$

subject to the normalization constant

$$\langle\psi|\psi\rangle = 1 \tag{5}$$

For the relativistic case the corresponding Dirac equation is to be solved. It is assumed that no electron current takes place at the boundary surface defined by the Wigner-Seitz radius R and the wave function should satisfy the boundary condition

$$\psi(r) = 0 \qquad \text{at} \quad \mathrm{r = R} \tag{6}$$

Such boundary conditions can always be satisfied by choosing the basis sets appropriately. We represent the radial part of the orbital

$$\psi(r) = (R - r)\chi(r) \tag{7}$$

where $\chi(r)$ is a linear combination of Slater type orbitals (STO)

$$\chi(r) = \sum_i C_i r^{n_i} e^{-\rho_i r} \tag{8}$$

Since the analytical solution of Hydrogen like problem in a plasma is difficult we adopt the basis set expansion technique for obtaining the energy of the ground state in a plasma environment. The non linear parameters n_i and ρ_i here are preassigned and the linear coefficients are determined from the solution of the generalized eigenvalue equation

$$\mathbf{H}_0\ \mathbf{C} = E_0\ \mathbf{S}\ \mathbf{C} \tag{9}$$

which yields the ground state energy at different plasma coupling strengths which are functions of the plasma parameters. All the integrals are to be evaluated at finite domain radius R. For the relativistic case a numerical evaluation of the energies is sought using Dirac Hamiltonian and standard relativistic program package as developed by Fritzsche *et al.* [25].

In addition to evaluation of the ground state energies at different plasma coupling strengths we have adopted the applications of linear response theory under an external time dependent perturbation [21, 22, 23, 24] for estimating the low lying excitation energies with a view to calculate the spectral line positions under plasma environment.

To be more specific we apply a harmonic perturbation on the system

$$H'(\mathbf{r}, t) = g(\mathbf{r})e^{-i\omega t} + g^{\dagger}(\mathbf{r})e^{i\omega t} \tag{10}$$

where g($\mathbf{r}$) is an one particle perturbation, currently of dipolar form. The external perturbation changes the ground state wave function ψ and the perturbed wave functions can be evaluated through the optimization of a variational functional [26]

$$J(\phi) \quad = \quad \frac{1}{T}\int_0^T dt \frac{< \phi \mid H_0 + H' - i\frac{\partial}{\partial t} \mid \phi >}{< \phi \mid \phi >} \tag{11}$$

with

$$\delta J(\phi) = 0 \tag{12}$$

The optimization is carried out with respect to linear variation parameters introduced in function ϕ. The basis sets for the perturbed functions are similar to that given by Equations (7) and (8) with different linear and non linear parameters. The functional has poles at certain frequency ω, the positions of which indicate the singly excited states of the system. One can extract the transition properties from a study of the pole positions [21]. A discussion of the results is given in the next section.

3 Results and Discussions

The effect of strongly coupled plasma on the orbital energy and low lying excited states C^{5+}, Al^{12+} and Ar^{17+} has been analyzed in details using IS model within non relativistic as well as relativistic theory. The particular ions have been chosen as laser produced plasma experiments in such systems exist [10, 11, 12] and spectral lines of Lyman lines originating in plasma environments have been reported. Our aim is to see the reliability of the IS model of the plasma in predicting the experimentally observed lines of the Lyman series. The shifts can always be estimated from the free line positions. The orbital energies for different plasma coupling strengths have been obtained from the solution of the generalized eigenvalue Equation (10) with respect to a limited basis set composed of linear combination of STO's. For C^{5+} ion we have chosen only a two parameter representation for the ground orbital and its reliability has been tested by comparing the eigen energy for the free systems. For Al^{12+} and Ar^{17+} we have chosen four parameter representation for the same. To study the excitation energies and transition wavelengths under plasma we used a twelve parameter representation of the first order perturbed orbitals for C^{5+} while an 8 parameter representation was adopted for Al^{12+} and Ar^{17+}. For the case of Al^{12+} and Ar^{17+} the results for our detailed investigations using IS model with different electron densities have been displayed in Tables 1 and 3. We have considered the behavior of the ground state orbital energy and the transition energy to first three dipole allowed excited states $2p$, $3p$ and $4p$. The energy shifts have been calculated for Al^{12+} while for Ar^{17+}, the wavelengths for the free as well as those in presence of plasma have been reported. This is because the data on the laser produced experiments on plasma for Al^{12+} [10] and Ar^{17+} [12] have been given accordingly. We wish to have an overall idea also about how the energy levels behave in case of Debye type plasma with spherical confinement. Here the effective potential is given by [4]

$$V_{eff}(r) = -\frac{Ze^{-\mu r}}{r} \tag{13}$$

where Z is the nuclear charge and μ is the Debye screening parameter given by

$$\mu = \left[\frac{4\pi(1+Z)n}{\kappa T}\right]^{\frac{1}{2}} \tag{14}$$

μ is a function of the temperature T and number density n of the plasma electrons. One can simulate a large number of plasma conditions by properly choosing n and T. Using the potential function given by Equation (13) with a given parameter μ, one can proceed in the same way as is being done in the strongly coupled plasma model to study the behavior of orbital energies and excitation properties. In such calculations we have chosen the plasma temperature T as reported in the experimental papers [11, 12] and varies the electron density n to get the screening parameters μ. For each μ value we have chosen the radius of confinement as $R = \frac{1}{\mu}$ which effectively gives the Debye sphere of influence. The spatial confinement with respect to the Debye radius is incorporated in the numerical calculations in exactly the same way as is being done for the Ion Sphere (IS) model. Such results have been displayed in Tables 2 and 4 for the respective cases of Al^{12+} and Ar^{17+}. The number of parameters for the ground and excited state functions are identical in the Debye plasma and in the IS models. In Tables 1 to 4 the transition energies from the $1s \rightarrow 2p$, $3p$ and $4p$ states have been reported for the cases only in which the excited state is bound. As soon as the transition energy exceeds that of the ionization energy for increased plasma strength, it goes in the continuum and such cases have not been displayed in the Tables. Experimental shift for the Lyman α (Ly_α) line for Al^{12+} with estimated electron density $n \sim (5-10) \times 10^{23}$/cc and temperature $T \sim 300$ eV is given by 3.7 ± 0.7 eV [12]. Our calculation using IS model at $n = 2.5 \times 10^{24}$/cc yields a value 3.41 eV whereas a quantum mechanical calculations of Nguyen *et al.* [27] based on collision theory yields a value 3.5 eV at $n = 8 \times 10^{23}$/cc and $T \sim 300$ eV. Figure 1 shows the general trend of the transition energy $1s \rightarrow 2p$ for Al^{12+} against the Ion Sphere radius R with non relativistic and relativistic models. For the relativistic case weighted average of the $p_{\frac{3}{2}}$ and $p_{\frac{1}{2}}$ state energies have been reported all throughout. It appears that the relativistic results differ only at higher plasma electron densities. In Figure 2 we plotted the non relativistic and relativistic transition wavelengths $1s \rightarrow 2p$, $3p$ and $4p$ against IS plasma density for Ar^{17+}. The relativistic effects are little more pronounced here as the nuclear charge Z is larger. Figure 3 displays a comparison of our calculated results for the transition wavelengths for Ar^{17+} using non relativistic as well as relativistic methods within Ion Sphere (IS) model and spatially confined Debye screening model with the laser plasma experimental data. The experimental data are in reasonable agreement with the calculated theoretical results. The laser plasma experiment by Nantel *et al.* [10] yields data on Hydrogen and Helium like spectra of C under strong plasma with estimated density of $n = 1.5 \times 10^{21}$/cc and temperature 48 eV. We have performed non relativistic and relativistic estimates of the positions of Lyman lines of C^{5+} using the Ion Sphere (IS) model at experimental density and spatially confined Debye plasma model at the same density and temperature. In Figure 4 we displayed our results along with those obtained by Nantel *et al.* [10]. We observed very reasonable fitting with the experimental lines positions for the Lyman transitions $1s \rightarrow 2p$, $3p$, $4p$, $5p$ and $6p$. It appears that with IS model non relativistic and relativistic estimates agree very well while there are little variations with confined Debye plasma model.

4 Conclusion

From the analysis of the calculated data by using IS and Debye models one can conclude that IS model, though simple, yields very reasonable theoretical estimates of spectral line positions and shifts of the spectral lines obtained from laser produced plasmas. It can be a viable method for the understanding of the experimental observations on strongly coupled plasmas obtained in laboratory and astrophysics.

5 Acknowledgement

The authors are thankful to AvH foundation for financial assistance towards mutual visits of Indian and German scientists. The financial assistance from the Department of Science and Technology (DST), Govt. of India under research grant no. SR/S2/LOP-05/2005 is gratefully acknowledged.

References

[1] B. Tabbert, H. Günther, G. zu Putlitz, J. Low. Temp. Phys. **109**, 653 (1997)

[2] W. Jaskolski, Phys. Rep. **271**, 1 (1996)

[3] J. P. Connerade, V. K. Dolmatov, P. A. Lakshmi, J. Phys. B, At. Mol. Opt. Phys., **33**, 251 (2000)

[4] A. I. Akhiezer, I. A. Akhiezer, R. A. Polovin, A. G. Sitenko, K. N. Stepanov: *Plasma Electrodynamics*; Vol. **1**; *linear response theory*, Oxford, Pergamon, 1975.

[5] S. Ichimaru, Rev. Mod. Phys. **54**, 1017 (1982)

[6] B. A. Hammel *et al.*, Phys. Rev. Lett. **70**, 1263 (1993)

[7] L. DaSilva, A. Ng, B. K. Godwal, G. Chiu, F. Cottet, M. C. Richardson, P. A. Jaanimagi, Phys. Rev. Lett. **62**, 1623 (1989); A. Djaoui *et al.*, Plasma Phys. Controlled Fusion **31**, 111 (1989)

[8] E. Leboucher-Dalimier *et al.*, J. Quant. Spectrosc. Radiat. Transfer **51**, 187 (1994)

[9] J. Workman *et al.*, Appl. Phys. Lett. **70**, 312 (1997)

[10] M. Nantel, G. Ma, S. Gu, C. Y. Cote, J. Itatani, D. Umstadter, Phys. Rev. Lett. **80**, 4442 (1998)

[11] N. C. Woolsey, B. A. Hammel, C. J. Keane, C. A. Back, J. C. Moreno, J. K. Nash, A. Calisti, C. Mosse, R. Stamm, B. Talin, A. Asfaw, L. S. Klein, R. W. Lee, Phys. Rev. E **57**, 4650 (1998)

[12] A. Saemann, K. Eidmann, I. E. Golovkin, R. C. Mancini, E. Andersson, E. Forster, K. Witte, Phys. Rev. Lett. **82**, 4843 (1999)

[13] J. C. Stewart, Jr. K. D. Pyatt, Astrophys. J. **144**, 1203 (1966)

[14] B. F. Rozsnyai, Phys. Rev. A **43**, 3035 (1991)

[15] D. Ray, Phys. Rev. E **62**, 4126 (2000)

[16] Y. D. Jung, Eur. Phys. J. D **7**, 249 (1999) and references therein.

[17] H. R. Griem, (a) Phys. Rev. A **15**, 2943 (1988); (b) Spectral Line Broadening by Plasmas; Academic Press, New York, 1974.

[18] J. Seidel, S. Arndt, W. D. Kraeft, Phys. Rev. E **52**, 5387 (1995)

[19] S. Skupski, Phys. Rev. A **21**, 1316 (1980)

[20] U. Gupta, A. K. Rajagopal, Phys. Rept. **87**, 259 (1982)

[21] B. Saha, P. K. Mukherjee, G. H. F. Diercksen, Astron. Astrophys. **396**, 337 (2002)

[22] A. N. Sil, B. Saha, P. K. Mukherjee, Int. J. Quantum Chem. **104**, 903 (2005)

[23] B. Saha, P. K. Mukherjee, D. Bielinska-Waz, Jacek Karwowski, J. Quant. Spectrosc. Radiat. Transfer **92**, 1, (2005); ibid, **78**, 131 (2003)

[24] A. N. Sil, P. K. Mukherjee, Int. J. Quantum Chem. **106**, 465 (2006)

[25] S. Fritzsche, J. Electr. Spec. Rel. Phenom. **114-116**, 1155 (2001); Phys. Scr. **T100**, 37 (2002)

[26] P. O. Löwdin, P. K. Mukherjee, Chem. Phys. Lett. **14**, 1 (1972)

[27] H. Nguyen, M. Koenig, D. Benredjem, M. Caby, G. Coulaud, Phys. Rev. A **33**, 1279 (1986)

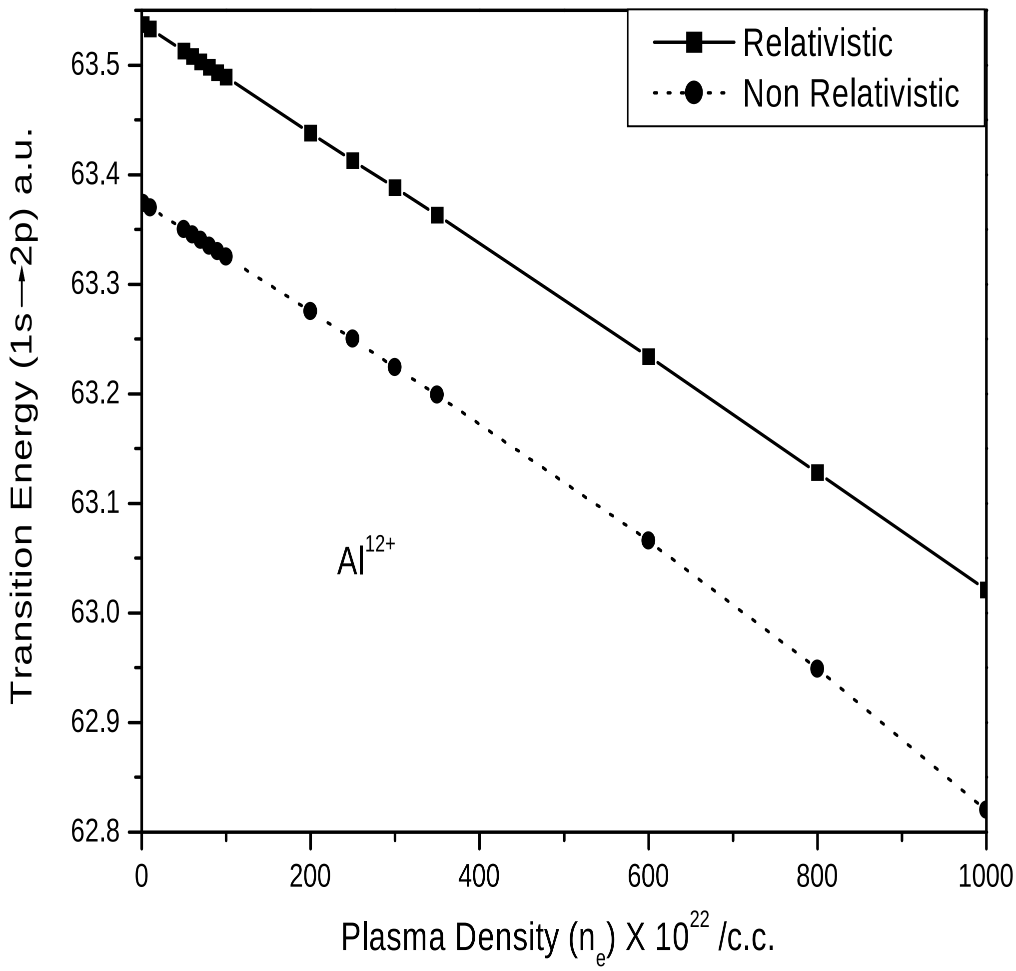

Figure 1: Plot of the relativistic and non relativistic transition energy ($1s \rightarrow 2p$) (a.u.) obtained by using IS model against plasma electron density (/cc) for Al^{12+}.

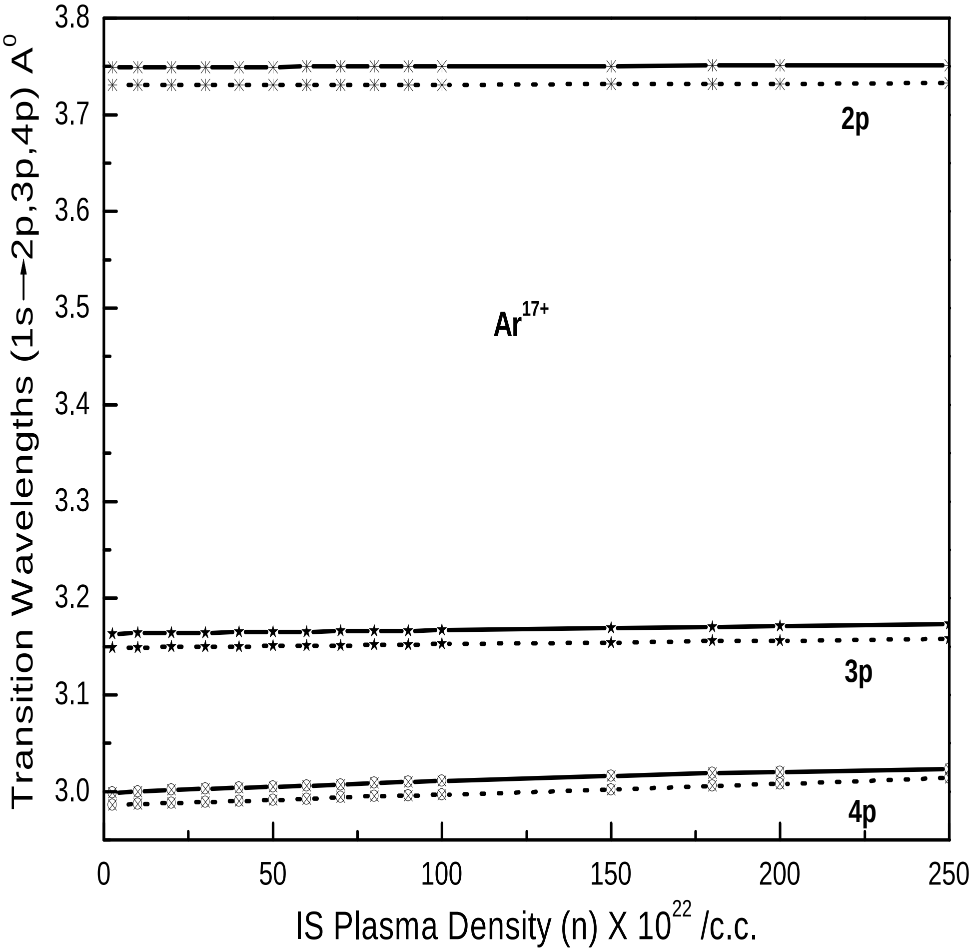

Figure 2: Plot of the relativistic (dotted line with symbols) as well as non relativistic transition (solid line with symbols) wavelength ($1s \rightarrow 2p, 3p, 4p$) (Å) obtained by using IS model against plasma electron density (/cc) for Ar^{17+}.

Table 1: **Relativistic & non-relativistic transition energy of Al^{12+} for different Ion-Sphere (IS) radius.**

Ion-sphere Radius (a.u.)	Plasma Density n_e/c.c.	Orb Ener (a.u.) Rel	Orb Ener (a.u.) Non-Rel	Transition Scheme	Transition energy (a.u.) Rel	Transition energy (a.u.) Non-Rel	Energy shift (eV) Rel	Energy shift (eV) Non-Rel
∞		84.69	84.50	1s→2p	63.53747	63.37500		
				→3p	75.28958	75.11111		
				→4p	79.40327	79.21875		
9.9	1.99(+22)	82.8729	82.6819	1s→2p	63.53715	63.37401	0.0087	0.0269
				→3p	75.28855	75.10482	0.0280	0.1709
				→4p	79.38251	79.19697	0.5649	0.5927
5.7822	1.0(+23)	81.5785	81.3876	1s→2p	63.53319	63.37003	0.1165	0.1352
				→3p	75.26206	75.09233	0.7489	0.5108
				→4p	79.29516	79.10701	2.9418	3.0406
3.38146	5.0(+23)	79.3706	79.1796	1s→2p	63.51337	63.35014	0.6558	0.6765
				→3p	75.12798	74.98010	4.3974	3.5647
				→4p	78.86261	78.70955	14.7121	13.8540
3.18207	6.0(+23)	79.0376	78.8467	1s→2p	63.50841	63.34516	0.7908	0.8120
				→3p	75.09388	74.94203	5.3253	4.6006
				→4p	78.75720	78.66120	17.5805	15.1717
3.0227	7.0(+23)	78.7399	78.5489	1s→2p	63.50344	63.34018	0.9260	0.9475
				→3p	75.05951	74.90371	6.2605	5.6434
2.89111	8.0(+23)	78.4694	78.2784	1s→2p	63.49847	63.33519	1.0612	1.0833
				→3p	75.02489	74.86516	7.2026	6.6924
2.7798	9.0(+23)	78.2206	78.0297	1s→2p	63.49349	63.33019	1.1968	1.2193
				→3p	74.98993	74.82618	8.1539	7.7531
2.68386	1.0(+24)	77.9897	77.7987	1s→2p	63.48851	63.32519	1.3323	1.3554
				→3p	74.95463	74.78648	9.1145	8.8334
2.13018	2.0(+24)	76.2519	76.0610	1s→2p	63.43847	63.27495	2.6939	2.7225
				→3p	74.58295	74.31376	19.2284	21.6967
1.97749	2.5(+24)	75.6022	75.4113	1s→2p	63.41328	63.24965	3.3794	3.4109
				→3p	74.38536	74.03433	24.6051	29.3004
1.86089	3.0(+24)	75.0346	74.8437	1s→2p	63.38798	63.22420	4.0678	4.1035
				→3p	74.18693	73.75165	30.0046	36.9925
1.76768	3.5(+24)	74.5273	74.3364	1s→2p	63.36256	63.19856	4.7595	4.8012
				→3p	73.98516	73.47956	35.4951	44.3965
1.4770	6.0(24)	72.5370	72.3461	1s→2p	63.23364	63.06557	8.2676	8.4800
1.3419	8.0(24)	71.3210	71.1306	1s→2p	63.12816	62.94926	11.1379	11.5850
1.2457	1.0(25)	70.2961	70.1059	1s→2p	63.02080	62.82014	14.0593	15.0985

Table 2: **Relativistic & non-relativistic transition energy of Al^{12+} for different Debye Screening parameter and box radius.**

Ion	Plasma Density (/c.c.)	Temp. (eV)	Debye Para (a.u.)	Debye Sh Rad (a.u.)	Orbital Energy -E(a.u.)		Transition Scheme	Transition Energy (a.u.)		Energy Shift (eV)	
					Rel	Non-Rel		Rel	Non-Rel	Rel	Non-Rel
Al^{12+}	1.0(22)	300	0.154	6.50328	82.7066	82.5156	1s→2p	63.49789	63.33468	1.0770	1.0972
							3p	75.17195	74.99568	3.2009	3.1410
							4p	79.17590	78.98747	6.1871	6.2935
	1.5(22)	300	0.188	5.30991	82.2731	82.0823	1s→2p	63.47852	63.31529	1.6041	1.6248
							3p	75.11382	74.95165	4.7827	4.3391
							4p	79.07184	78.88048	9.0187	9.2048
	2.0(22)	300	0.217	4.59852	81.9048	81.7139	1s→2p	63.45912	63.29586	2.1320	2.1535
							3p	75.05604	74.90643	6.3550	5.5696
							4p	78.97013	78.77558	11.7863	12.0593
	2.5(22)	300	0.243	4.11304	81.5756	81.3847	1s→2p	63.43951	63.27621	2.6656	2.6882
							3p	74.99892	74.85465	7.9093	6.9786
							4p	78.86956	78.67419	14.5230	14.8182
	3.0(22)	300	0.266	3.75467	81.2852	81.0944	1s→2p	63.42043	63.25709	3.1848	3.2085
							3p	74.94271	74.79863	9.4388	8.5030
							4p	78.77459	78.58558	17.1073	17.2294
	3.5(22)	300	0.288	3.47615	81.0081	80.8173	1s→2p	63.40068	63.23729	3.7222	3.7473
							3p	74.88485	74.73743	11.0133	10.1684
							4p	78.67940	78.50974	19.6975	19.2932
	4.0(22)	300	0.308	3.25164	80.7568	80.5661	1s→2p	63.38146	63.21803	4.2453	4.2714
							3p	74.82883	74.67665	12.5377	11.8223
							4p	78.58756	78.45786	22.1966	20.7049
	4.5(22)	300	0.326	3.06568	80.5311	80.3404	1s→2p	63.36315	63.19967	4.7435	4.7710
							3p	74.77574	74.61846	13.9823	13.4057
							4p	78.51635	78.43443	24.1343	21.3424
	5.0(22)	300	0.344	2.90836	80.3059	80.1152	1s→2p	63.34388	63.18036	5.2679	5.2964
							3p	74.72022	74.55784	15.4931	15.0553
							4p	78.45252	78.43180	25.8712	21.4140

Table 3: **Relativistic & non-relativistic transition energy of Ar^{17+} for different Ion-Sphere (IS) radius.**

Ion	Plasma Density (/c.c.)	IS Radius (a.u.)	Orbital Energy -E(a.u.)		Transition Scheme	Transition Energy (a.u.)		Transition Wave length (Å)	
			Rel	Non-Rel		Rel	Non-Rel	Rel	Non-Rel
Ar^{17+}	9.54(20)	30.0	161.8549	161.1500	1s→2p	122.10220	121.49997	3.7305	3.7490
					3p	144.66130	143.99982	3.1488	3.1633
					4p	152.56180	151.87442	2.9857	2.9992
	2.58(22)	10.0	160.1549	159.4500	1s→2p	122.10153	121.49929	3.7306	3.7491
					3p	144.65685	143.99535	3.1489	3.1633
					4p	152.54681	151.86477	2.9860	2.9994
	1.0(23)	6.4941	158.7785	158.0736	1s→2p	122.09966	121.49741	3.7306	3.7491
					3p	144.64459	143.98306	3.1492	3.1636
					4p	152.50553	151.81798	2.9868	3.0004
	2.0(23)	5.1543	157.7581	157.0533	1s→2p	122.09709	121.49482	3.7307	3.7492
					3p	144.62769	143.96644	3.1495	3.1640
					4p	152.44872	151.75973	2.9879	3.0015
	3.0(23)	4.5027	157.0425	156.3376	1s→2p	122.09452	121.49223	3.7308	3.7493
					3p	144.61075	143.95059	3.1499	3.1643
					4p	152.39194	151.70093	2.9891	3.0027
	4.0(23)	4.0190	156.3612	155.7680	1s→2p	122.09138	121.48964	3.7309	3.7494
					3p	144.59007	143.93565	3.1503	3.1647
					4p	152.32277	151.62842	2.9904	3.0041
	5.0(23)	3.7978	155.9918	155.2869	1s→2p	122.08937	121.48705	3.7309	3.7494
					3p	144.57679	143.92126	3.1506	3.1650
					4p	152.27847	151.58148	2.9913	3.0050
	6.0(23)	3.5738	155.5713	154.8665	1s→2p	122.08680	121.48447	3.7310	3.7495
					3p	144.55975	143.90649	3.1510	3.1653
					4p	152.22179	151.52097	2.9924	3.0062
	7.0(23)	3.3948	155.1954	154.4906	1s→2p	122.08422	121.48187	3.7311	3.7496
					3p	144.54269	143.89068	3.1514	3.1657
					4p	152.16513	151.46022	2.9935	3.0074

Ion	Plasma Density (/c.c.)	IS Radius (a.u.)	Orbital Energy -E(a.u.)		Transition Scheme	Transition Energy (a.u.)		Transition Wave length (Å)	
			Rel	Non-Rel		Rel	Non-Rel	Rel	Non-Rel
	8.0(23)	3.2470	154.8538	154.1490	1s→2p	122.08165	121.47928	3.7312	3.7497
					3p	144.52559	143.87384	3.1517	3.1660
					4p	152.10852	151.39962	2.9946	3.0086
	9.0(23)	3.1220	154.5396	153.8348	1s→2p	122.07908	121.47669	3.7313	3.7498
					3p	144.50846	143.85638	3.1521	3.1664
					4p	152.05193	151.33965	2.9957	3.0098
	1.0(24)	3.0143	154.2480	153.5431	1s→2p	122.07650	121.47410	3.7313	3.7498
					3p	144.49129	143.83861	3.1525	3.1668
					4p	151.99539	151.28082	2.9969	3.0110
	1.5(24)	2.6332	153.0251	152.3203	1s→2p	122.06361	121.46113	3.7317	3.7502
					3p	144.40493	143.74921	3.1544	3.1688
					4p	151.71395	151.01987	3.0024	3.0162
	1.8(24)	2.4780	152.4192	151.7144	1s→2p	122.05588	121.45334	3.7320	3.7505
					3p	144.35266	143.69573	3.1555	3.1699
					4p	151.54573	150.90012	3.0057	3.0186
	2.0(24)	2.3924	152.0519	151.3471	1s→2p	122.05071	121.44814	3.7321	3.7506
					3p	144.31763	143.66004	3.1563	3.1707
					4p	151.43565	150.83746	3.0079	3.0199
	2.5(24)	2.2209	151.2303	150.5256	1s→2p	122.03780	121.43514	3.7325	3.7510
					3p	144.22930	143.57026	3.1582	3.1727
					4p	151.15811	150.73922	3.0135	3.0218

Table 4: **Relativistic & non-relativistic transition energy of Ar^{17+} for different Debye Screening parameter and box radius.**

Ion	Plasma Density (/c.c.)	Temp (eV)	Debye para (a.u.)	Debye Radius (a.u.)	Orbital Energy -E (a.u.)		Tran Sch	Transition Energy (a.u.)		Transition Wave length (Å)	
					Rel	Nol-Rel		Rel	Nol-Rel	Rel	Nol-Rel
Ar^{17+}	1.0(23)	1000	0.3103	3.2230	157.1904	156.4865	1s→2p	121.94107	121.33840	3.7355	3.7540
							3p	144.17601	143.52411	3.1594	3.1737
							4p	151.67941		3.0031	
	5.0(23)	1000	0.6938	1.4414	150.5664	149.8640	1s→2p	121.33281	120.72769	3.7542	3.7730
							3p	142.49773	141.51795	3.1966	3.2187
							4p	150.25318		3.0316	
	1.0(24)	1000	0.9812	1.0192	145.7360	145.0367	1s→2p	120.61125	119.98983	3.7767	3.7962
							3p	141.17721	138.52859	3.2265	3.2882
	5.0(24)	1000	2.1939	0.4558	126.5337	125.8566	1s→2p	116.71007	111.28980	3.9029	4.0930

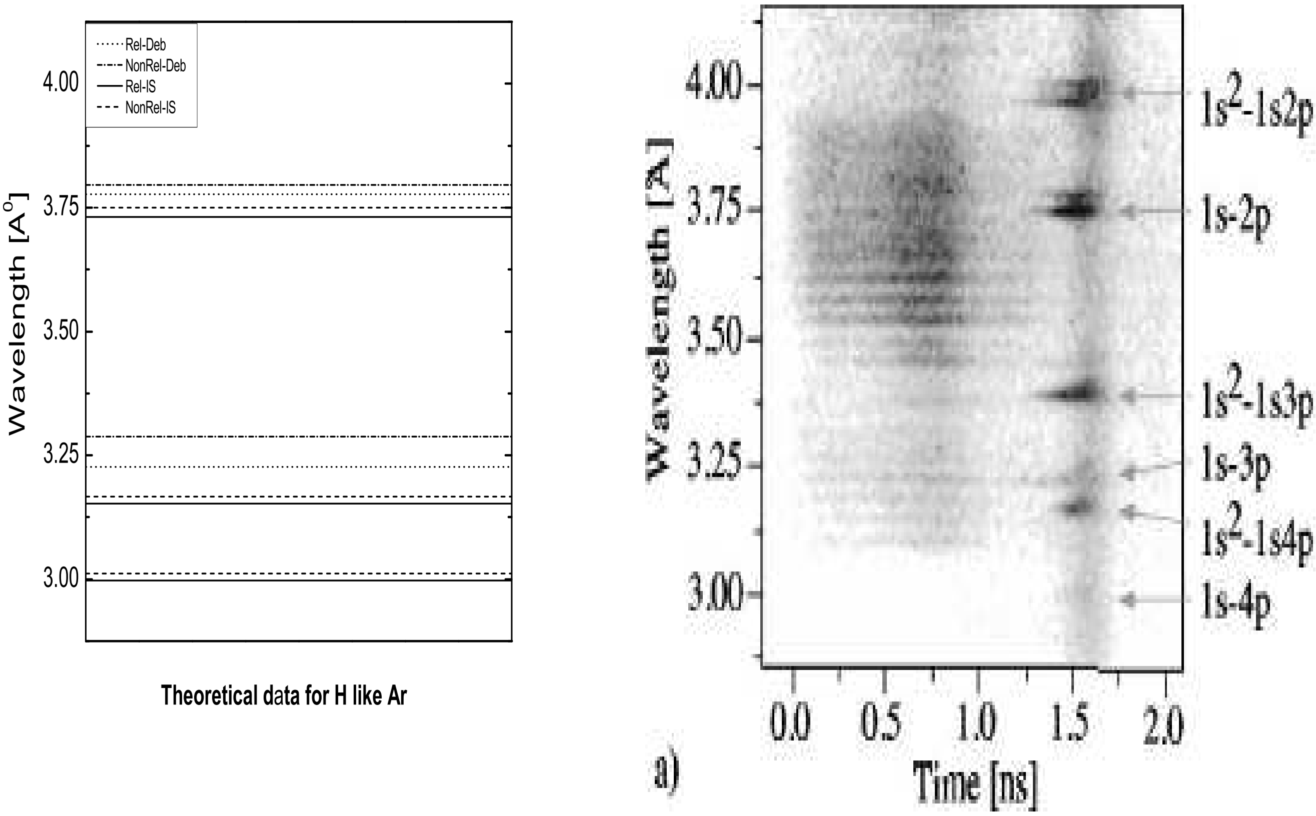

Figure 3: Comparison between the experimental results and that obtained theoretically by using Ion Sphere as well as Debye plasma model for $1s \rightarrow 2p, 3p, 4p$ transition wavelength (Å) of Ar^{17+}. The experimental figure has been taken from Ref. 11.

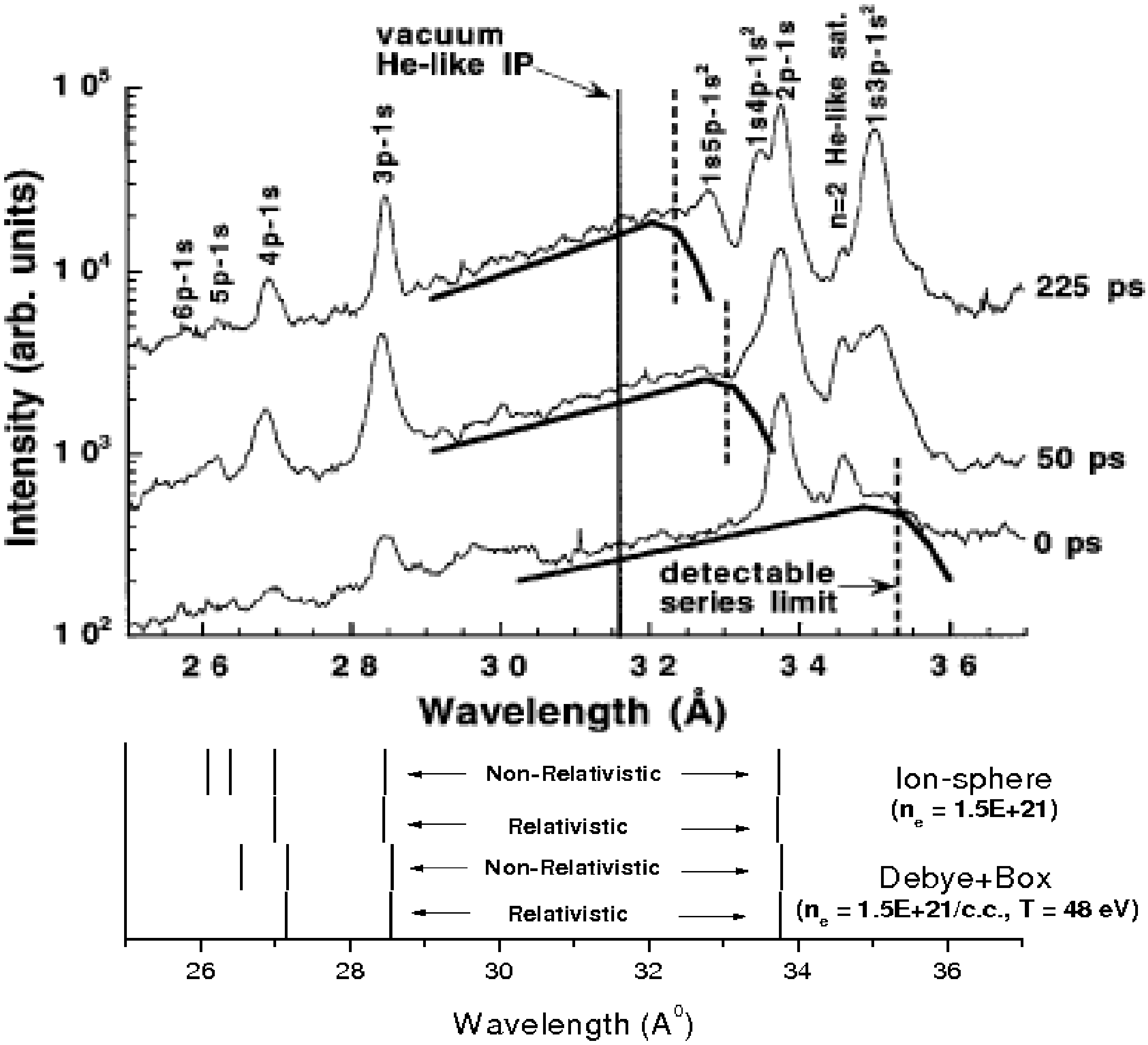

Figure 4: Comparison between the experimental results (C^{4+} and C^{5+}) and that obtained theoretically by using Ion Sphere as well as Debye plasma model for $1s \rightarrow 2p, 3p, 4p, 5p, 6p$ transition wavelength (Å) of Hydrogen like Carbon. The experimental figure has been taken from Ref. 10.